Heliyon 9 (2023) e18119

Contents lists available at ScienceDirect

Heliyon

journal homepage: www.cell.com/heliyon

Physicochemical characterization of biological and synthetic forms of two lipid A-based TLR4 agonists

Gang Hu [a], David J. Varisco [b], Sayan Das [b], C. Russell Middaugh [a], Francesca Gardner [b], Robert K. Ernst [b], Wendy L. Picking [a,c], William D. Picking [a,c,d,*]

[a] Department of Pharmaceutical Chemistry, University of Kansas, Lawrence, KS 66047, USA
[b] Department of Microbial Pathogenesis, University of Maryland, Baltimore, MD 21201, USA
[c] Department of Veterinary Pathobiology, University of Missouri, Columbia, MO 65211, USA
[d] Bond Life Sciences Center, University of Missouri, Columbia, MO 65211, USA

ARTICLE INFO

Keywords:
Lipid a
Adjuvant
TLR4 agonist
Bacterial enzymatic combinatorial chemistry (BECC)
Monophosphoryl lipid a

ABSTRACT

Toll-like receptor (TLR) agonists are recognized as potential immune-enhancing adjuvants and are included in several licensed vaccines. Monophosphoryl lipid A (MPL®, GlaxoSmithKline) is one such TLR4 agonist that has been approved for use in human vaccines, such as Cervarix and Shingrix. Due to the heterogeneous nature of biologically derived MPL and the need for safer and more potent adjuvants, our groups have developed the novel TLR4 agonist candidates, BECC438 and BECC470 using the Bacterial Enzymatic Combinatorial Chemistry (BECC) platform. BECC438 and BECC470 have been included in studies to test their adjuvant potential and found to be effective in vaccines against both viral and bacterial disease agents. Here, we report detailed biophysical characterization of BECC438 and BECC470 purified from a biological source (BECC438b and BECC470b, respectively) and synthesized chemically (BECC438s and BECC470s, respectively). Both BECC438s and BECC470s have identical acyl chain configurations, BECC438s is bis-phosphorylated and BECC470s is mono-phosphorylated with the removal of the 4′ phosphate moiety. We determined the phase transition temperatures for the acyl chains of BECC438b and BECC470b and found them to be different from those exhibited by their synthetic counterparts. Furthermore, the phosphate groups of BECC438b and BECC470b are more highly hydrated than are those of BECC438s and BECC470s. In addition to exploring the BECC molecules' biophysical features in aqueous solution, we explored potential formulation of BECC438 and BECC470 with the aluminum-based adjuvant Alhydrogel and as part of an oil-in-water emulsion (Medimmune Emulsion or ME). All of the lipid A analogues could be fully absorbed to Alhydrogel or incorporated onto ME. Surprisingly, the BECC470s molecule, unlike the others, displayed a nearly baseline signal when monitored using a Limulus amebocyte lysate (LAL) endotoxin detection system. Despite this, it was shown to behave as an agonist for human and mouse TLR4 when tested using multiple cell-based systems. This work paves the way for further formulation optimization of two chemically defined TLR4 agonists that are showing great promise as vaccine adjuvants.

* Corresponding author. Department of Veterinary Pathobiology, University of Missouri, Columbia, MO 65211, USA.
E-mail addresses: ganghu@ku.edu (G. Hu), pickingw@missouri.edu (W.D. Picking).

https://doi.org/10.1016/j.heliyon.2023.e18119
Received 12 January 2023; Received in revised form 19 June 2023; Accepted 7 July 2023
Available online 8 July 2023

1. Introduction

Vaccination has significantly reduced morbidity and mortality caused by bacterial and viral infections worldwide, however, the development of new and effective vaccines against infectious diseases continues to be an urgent need. With the growing use of protein subunit and conjugate vaccines that have strong safety profiles, it is critical to identify effective immunostimulatory adjuvants to enhance the resulting immune response. Unfortunately, relatively few adjuvants have been approved by FDA for use in human vaccines. Bacterially derived monophosphoryl lipid A (MPL®) is a potent TLR4 agonist and was the first of several families of TLR ligands to obtain FDA approval and is in the shingles vaccine Shingrix, the human papillomavirus (HPV) vaccine Cervarix and the hepatitis B virus (HBV) vaccine Fendrix [1–4]. As a well-studied TLR4 agonist, MPL promotes a Th1 (cellular)-biased immune response [2,5], however, MPL is a heterogeneous preparation from multiple congeners of lipid A, which results in compositional difference between batches [6]. To overcome the congener distribution of MPL, a synthetic variant of MPL termed phosphorylated hexa-acyl disaccharide (PHAD®) was produced and tested in clinical trials [7–10]. To identify novel and improved MPL analogues and overcome product heterogeneity with more potent immune protection, Bacterial Enzymatic Combinatorial Chemistry (BECC) was used to rapidly generate novel lipid A structures with adjuvant potential and low toxicity in an attenuated *Yersinia pestis* (*Yp*) isolate [11]. Among the BECC molecules produced, two BECC molecules, BECC438b and BECC470b, exhibited promising adjuvant properties as compared to MPL and PHAD [11] (see Suppl. Fig. S1). BECC438b and BECC470b have been tested as vaccine adjuvants in multiple experimental vaccine models against infectious disease including *Yersinia pestis* (plague) [12], *Pseudomonas aeruginosa* [13], HPV [14], influenza-A (flu) [15] and SARS-CoV-2 [16]. In some of those studies, a higher magnitude and more balanced production of antibody isotypes IgG1 and IgG2 were elicited when BECC438b or BECC470b was used in the formulation. This optimal antibody response was durable and maintained for 50 weeks or more post-vaccination and was part of a balanced Th1/Th2 response [12,15]. Furthermore, in flu studies BECC470b allowed for antigen sparing doses of a recombinant HA (rHA) protein and reduced the repeated dosing for vaccination [15].

To overcome the heterogeneity related with biological production of BECC438b and BECC470b, chemically synthesized versions were produced (BECC438s and BECC470s). Both BECC438s and BECC470s are hexa-acylated lipid A structures that are bis- or monophosphorylated, respectively with BECC470s lacking the 4' phosphate moiety, as compared to the 1 position of MPL and PHAD. The advantage of synthetic BECC438s and BECC470s over their biological counterparts is that every step the synthesis is traceable, scalable, and GMP production is achievable based on the established protocols; however, a detailed biophysical characterization of these lipid A analogues is still lacking.

In the present study, we conducted a comprehensive physicochemical analysis of BECC438b and BECC470b, from their biological *Y. pestis* source, for comparison with their synthetic counterparts BECC438s and BECC470s. We determined the phase transition temperature from gel to liquid crystalline phase for each BECC form using Fourier-transform infrared (FTIR) spectroscopy and differential scanning calorimetry (DSC). We then compared the relative particle sizes and the hydration states of the phosphate groups for these lipid A analogues. Finally, we performed a detailed study of these lipid A analogues in different formulations, including alone in aqueous solution, co-formulated with the aluminum-based adjuvant Alhydrogel (an AS04 biosimilar) and as part of a squalene-containing oil-in-water emulsion (AS03 biosimilar). An understanding of the physicochemical properties of these novel lipid A analogues will provide an unprecedented level of understanding how they behave in future vaccine formulations relative to less well defined TLR4 agonists and how the distinct properties of each may allow it to be tailored toward specific types of vaccine formulations (e.g. targeting viral or bacterial vaccine targets).

2. Materials and methods

2.1. Materials

L-histidine, 3-(*N*-morpholino)propanesulfonic acid (MOPS), triethylamine, and monophosphoryl lipid A (MPL) were purchased from Sigma-Aldrich (St. Louis, MO). Squalene was purchased from Echelon Biosciences (Salt Lake City, UT). Sucrose was purchased from Pfanstiehl Laboratories (Waukegan, IL). Polysorbate 80 was purchased from Fluka. Alhydrogel 2% was purchased from Brenntag Biosector A/S (Frederikssund, Denmark). The synthetic monophosphoryl lipid A analogue PHAD was purchased from Avanti Polar Lipids.

2.2. BECC438 and BECC470 purification and syntheses

BECC438b and BECC470b were purified from their corresponding *Y. pestis* KIM6+ strains as has been described in great detail previously [11,12]. The strain was cultured at 26 °C for 18 h to an OD600 of 1.0–1.4. After collecting the cells by centrifugation, the lipooligosaccharide (LOS) was extracted from the pellet using the double hot phenol method followed by three 2:1 (vol/vol) chloroform-methanol washes [11] and removal of contaminating small proteins. The extracted LOS samples were suspended in a 10 mM Tris-Cl buffer, pH 7.4, and digested for 4 h at 37 °C with 100 μg/mL DNase and 25 μg/mL RNase to remove all nucleic acid as determined by the conventional methods used in the Ernst laboratory. The lipid A portion was then prepared by mild acid hydrolysis [11]. MALDI-TOF mass spectrometry was used to confirm the structure of extracted BECC438b and BECC470b. Chemically synthesized BECC438s and BECC470s were prepared using proprietary methods and was analyzed to be more than 99% pure. Neither synthetic BECC molecule was found to be toxic using a rabbit single dose acute toxicity model as determined by Labcorp. The BECC structures described (Suppl. Fig. S1) and disclosed in this report have been properly disclosed and described in issued patents and pending patent applications by the University of Maryland – Baltimore.

2.3. Preparation of aqueous formulations

Aqueous formulations of BECC438 or BECC470 were prepared as described previously [17]. Briefly, BECC438 or BECC470 was added to 0.5% (v/v) triethylamine solution and was solubilized by vortexing for 2 min. Aqueous MPL and PHAD were prepared using the same steps. The solutions then were heated in a 65 °C water bath for 5 min. To further ensure BECC438 or BECC470 dispersal into the aqueous solution, bath sonication was applied for 30 min. Finally, the pH of the solution was adjusted to 7.2–7.4 with 1.0 M HCl and the formulation was filtered through 0.22 μm syringe filter.

2.4. Dynamic light scattering (DLS)

Particle size for all formulations was determined using dynamic light scattering (DLS) on a Zetasizer Ultra from Malvern Instruments (Worcestershire, UK). For all the formulations measured, DLS measurements were conducted at least three times with three independent samples.

2.5. UV–vis spectroscopy

The absorption spectra of BECC438 (b and s), BECC470 (b and s), MPL, and PHAD at 0.1 mg/mL were collected using a UV/visible spectrophotometer from Agilent Technologies (Santa Clara, CA) equipped with a diode array detector. The absorption spectra were corrected for scattering contributions by subtraction of an extrapolation of the logarithm of the optical density in a non-absorbing region (350–400 nm) to the far UV region.

2.6. RiboGreen assay

Quant-it RiboGreen assay kit (Cat#R11490) was purchased from Thermo Fisher Scientific. When RiboGreen reagent binds to RNA, the excitation maximum and the emission maximum are ~500 nm and ~525 nm, respectively. Due to its extremely high sensitivity for RNA quantitation, as low as 1 ng/mL RNA in the sample can be measured, we utilized the RiboGreen assay to determine whether the UV-absorbing material in the BECC438b and BECC470b preparations contained small amounts of RNA contamination. Briefly, the RNA standard from 0 to 2.5 μg/mL were prepared first by dilution of 16 S ribosomal RNA (100 μg/mL) in TE buffer, and equal volume of RiboGreen reagent was mixed with the RNA standard. After incubation for 5 min at room temperature protected from light, the fluorescence intensity of the RNA standard was measured (excitation 480 nm, emission 520 nm). To determine the RNA content in BECC438b and 470 b, the samples were diluted in 5 or 10 fold in TE buffer and mixed with the equal volume of RiboGreen reagent, and the fluorescence intensity was measured. The RNA concentration in the biological BECC samples was estimated based on the RNA standard curves.

2.7. Fourier-transform infrared (FTIR) spectroscopy

For infrared measurements, 20 mM BECC438 and 20 mM BECC470 were prepared in 10 mM HEPES buffer at pH 7. The suspensions were heated at 70 °C in a water bath for 5 min and then cooled down to 4 °C for 10 min for three cycles [18,19]. The samples were stored at 4 °C prior to obtaining measurements. FTIR spectroscopic analysis was performed using a Tensor-27 FTIR spectrometer (Bruker, Billerica, MA) equipped with a Bio-ATR cell. The detector was cooled with liquid N_2 for 20 min prior to use, and the interferometer was purged continuously with N_2 gas. A total of 256 scans were recorded from 4000 to 900 cm^{-1} with a 4 cm^{-1} resolution. Buffer background spectra were collected and subtracted from the sample spectra. Atmospheric compensation and baseline adjustment were applied using OPUS V6.5 software (Bruker, Billerica, MA). Thermal transition experiments were performed with the temperature ramped from 25 °C to 95 °C at increments of 2.5 °C per step and an equilibration time of 2 min at each temperature. The thermal transition curves were constructed by plotting the frequency shift at 2850 cm^{-1} as a function of temperature. The absorption at 2850 cm^{-1} indicates the methylene symmetric (*sv*CH2) stretching mode [20,21].

2.8. Differential scanning calorimetry (DSC)

DSC was performed using a MicroCal VP-Capillary calorimeter (Malvern, UK) equipped with an autosampler. The temperature was ramped from 10 °C to 90 °C at a scan rate of 1 °C/min. The sample cell was equilibrated for 15 min at 10 °C at the beginning of each run using a filtering period of 16 s. Samples were loaded into a 96-well plate, which was sealed and placed inside a sample container maintained at 4 °C. Samples were buffer subtracted, baselined, and normalized. Apparent transition temperatures were calculated using a non2-state equilibrium model in Origin 7.0 (OriginLab).

2.9. Limulus amoebocyte lysate (LAL) assay

The LAL assays were conducted using the Endosafe nexgen-PTS from Charles River Laboratories (Walkersville, MD). The LAL assay is the most sensitive and specific method to detect and measure bacterial endotoxin [22–24]. The Endosafe-PTS/MCS cartridge and its interface with the reader have been designed to mimic currently licensed Endpoint Chromogenic and Kinetic Chromogenic Methods. The aqueous formulations were evaluated using the LAL assay according to the manufacturer's instructions. Briefly, samples were

diluted in endotoxin-free water and placed in a PTS/MCS cartridge to determine which dilution was suitable for endotoxin measurement. Once the dilution factor was determined, PTS/MCS measurements were taken in duplicate with each experiment performed three times. The criteria for a valid assay were an archived curve correlation coefficient of ≤ -0.98 and spike (positive product control) recovery of 50–200%. The final endotoxin value of the aqueous formulations was the average value of the duplicate measurements.

2.10. Cell culture and TLR4/NF-κB activation assay

THP-1 Dual cells (a human monocyte line) were cultured in RPMI 1640 (Gibco) supplemented with 10% heat-inactivated fetal bovine serum (FBS) (Gibco), 100 IU/mL penicillin, 100 μg/mL streptomycin, 1 mM sodium pyruvate, and 200 mM L-glutamine. THP-1 cells were then cultured with 50 nM vitamin D3 (Sigma-Aldrich) for 48 h to generate monocyte derived macrophages prior to stimulation. Other cell lines included RAW-Blue mouse macrophages, mTLR4 HEK-Blue cells (possessing a mouse TLR4 reporter system) and hTLR4-HEK-Blue cells (possessing a human TLR4 reporter system). All cell lines were obtained from Invivogen. These other cell lines were cultured with DMEM (Gibco) with the above supplements. Ligands were diluted in tissue culture media prior to stimulation. Supernatants were collected from cells 18 h after stimulation. The production of the secreted embryonic alkaline phosphatase (SEAP) reporter was detected using the Quanti-Blue fluorescent dye (Invivogen) according to the manufacturer's instructions. Data were graphed as the mean results ± standard deviations (SD) from biological duplicates and analyzed using GraphPad Prism (La Jolla, CA).

2.11. Particle characterization of alhydrogel (AH) formulations

The size distribution of Alhydrogel as a function of lipid A analogue adsorption was determined using a Malvern Mastersizer 3000 (Malvern Instruments). First, 6 mL of dH_2O was added to the sample chamber and a background measurement was taken. About 300 μl of Alhydrogel sample was injected for each measurement (Alhydrogel at 1 g/L) for a total light obscuration of ~10%. A refractive index of 1.57 was used for Alhydrogel in the Mie scattering calculations for size determination. Size distribution of different formulations were reported by volume. Each sample was an average of ten instrumental replicates. Three independent sample measurements were

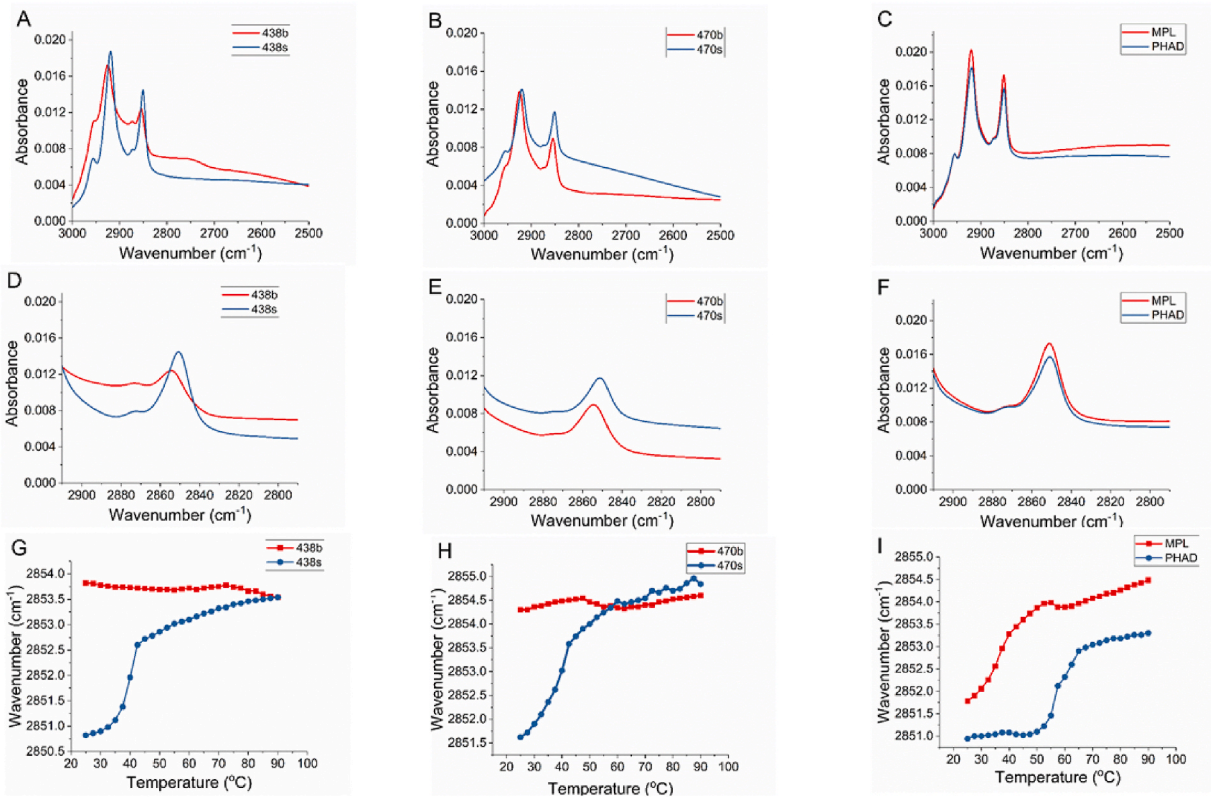

Fig. 1. FTIR spectral analysis of the six lipid A analogues. The spectra from 3000 to 2500 cm^{-1} for biological and synthetic BECC438 (A), biological and synthetic BECC470 (B), MPL (C), and PHAD (C) at 25 °C are shown. In order to show the peak positions of the symmetric stretching vibration of the methylene groups $_s\nu$ (CH2) around 2850 cm^{-1}more clearly, the spectra from 2910 to 2790 cm^{-1} for biological and synthetic BECC438 (D), biological and synthetic BECC470 (E), MPL (F), and PHAD (F) at 25 °C are also plotted. The peak positions of the symmetric stretching vibration of the methylene groups $_s\nu$ (CH2) were then monitored as a function of temperature from at 25 °C–90 °C for both forms of BECC438 (G), both forms of BECC470 (H), and MPL and PHAD (I).

performed. Zeta potential measurements were performed using a Malvern Zetasizer Ultra (Malvern Instruments). One mL of sample was placed in a plastic disposable capillary cell and zeta potential measured with a 632 nm laser in a 173° backscatter configuration. Each sample was diluted 50-fold into water and the final value was an average of six instrumental replicates. The measurement was performed for three independent samples to obtain a standard deviation.

2.12. Oil-in-water emulsion formulation

The Medimmune emulsion (ME) 2X stock contained 20 mM histidine pH 6.0, 10% sucrose, 4% squalene, and 1% polysorbate-80 was prepared according to a previously described protocol [25]. Initially, squalene and polysorbate-80 were mixed and sonicated to achieve homogenous mixing of the oil phase. The aqueous phase was then added to the oil phase. The mixture was homogenized with a Silverson L5M-A standard high-speed mixer at 7500 RPM for 10 min followed by 6 passages through a Microfluidics 110 P microfluidizer to generate the emulsion formulation. To make the ME-lipid A co-formulation, the oil phase was prepared by mixing 0.8 g of squalene, 0.2 g of polysorbate-80, and 4 mg of lipid A. The oil phase was sonicated in a water bath sonicator at 55 °C until the lipid A was completely re-suspended, to which 19 mL of aqueous phase to the oil phase, followed by homogenization and microfluidization. The high-speed homogenization was conducted for 10 min, and the mixture was subjected to microfluidization with LV1 microfluidizer as described above.

3. Results

3.1. Phase transition determined by FTIR

Biologically derived and synthetic BECC438 and BECC470 were analyzed and compared with respect to phase behavior and conformation using FTIR spectroscopy. MPL and PHAD represented comparators to the biologically- and synthetically-derived BECCs, respectively. One objective of the FTIR measurement was to determine the gel to liquid crystalline phase behavior of the acyl chains of BECC438 and BECC470. The phase change was evaluated by determining the symmetric stretching vibration of the methylene groups $_s\nu$ (CH2) at approximately 2850 cm^{-1}. The $_s\nu$ (CH2) band is relatively free from contributions of CH3 groups and is sensitive to the conformal disorder of trans methylene chains. A disordering of the conformations of the lipid structure is associated with an increase in this peak position [21]. The peak position of acyl chains of BECC438b and BECC470b at 25 °C is close to 2854 cm^{-1}, which is the characteristic of the symmetric stretching vibration of the methylene group $_s\nu$ (CH2) in a less ordered liquid-crystalline phase (Fig. 1A and B). In contrast, the peak position of the acyl chains of BECC438s and BECC470s is close to 2851 cm^{-1}, which is more characteristic of the symmetric stretching vibration for the methylene group $_s\nu$ (CH2) in a highly ordered gel phase (Fig. 1A and B). This observation is confirmed by the analysis of change of the peak position of $_s\nu$ (CH2) as a function of temperature. The peak position of the methylene group of the acyl chains of BECC438b and BECC470b did not change over the temperature ramp and remains at 2854 cm^{-1} (Fig. 1D and E), indicating there is no phase change for the acyl chains of BECC438b and BECC470b. In contrast, the peak position of BECC438s and BECC470s increased from 2851 to 2854 cm^{-1}during the temperature ramp (Fig. 1D & E), indicating a phase change for the acyl chains of BECC438s and BECC470s from a highly ordered gel phase to a randomly oriented liquid crystalline phase. The phase transition temperatures (T_c) of BECC438s and BECC470s were determined by taking the first derivative of the plots. The T_c values for BECC438s and BECC470s are 39.6 and 41.2 °C, respectively.

As a comparison, MPL and PHAD were also subjected to FTIR analysis. For MPL, the stretching vibration of the methylene groups showed the peak position at 2851.8 cm^{-1} rather than 2854 cm^{-1}, as was exhibited by BECC438b and 470 b or the 2851 cm^{-1} exhibited by the synthetic BECC molecules, indicating MPL is in a mixed phase with partial gel phase and partial liquid crystalline phase. Its synthetic counterpart PHAD showed peak position around 2851 cm^{-1}, indicating it is in a gel phase, which is similar to the peak position for BECC438s and BECC470s, however, PHAD has a much higher T_c value at 58.3 °C versus 36.3 °C for MPL. The T_c values for BECC438s and BECC470s were more like that seen for MPL rather than that seen for PHAD.

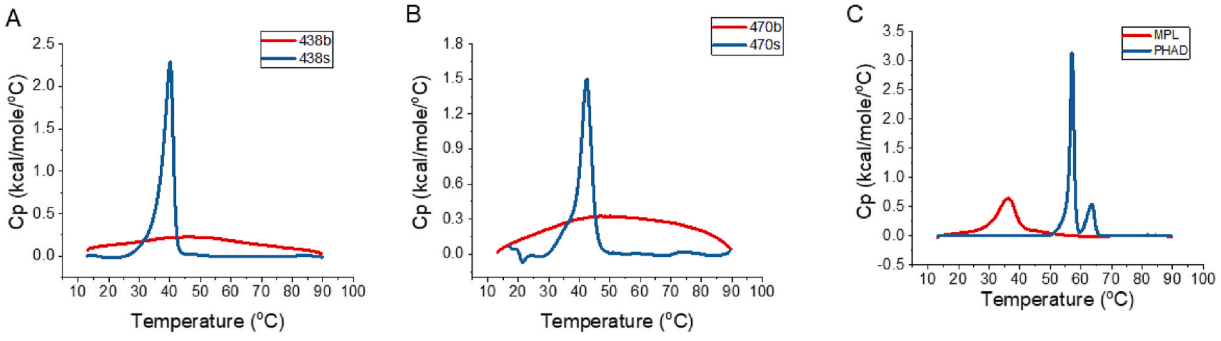

Fig. 2. DSC thermograms are shown for BECC438b and BECC438s (A), BECC470b and BECC470s (B), and MPL and PHAD (C). All of the synthetic analogues display sharper transitions than their biological counterparts.

3.2. Differential scanning calorimetry (DSC)

To determine the thermotropic phase behavior of lipids, DSC was used to study the thermal behavior of the biological and synthetic forms of BECC438 and BECC470. As shown in Fig. 2, neither BECC438b nor BECC470b demonstrated a clear phase transition. In contrast, BECC438s and BECC470s exhibited sharp transitions at about 40 °C. These data corroborate the FTIR results presented above that BECC438b and BECC470b are in a disordered fluid-like state even at low temperature, while BECC438s and BECC470s appear to be in a gel phase with the acyl chains fully extended and closely packed. DSC experiments were also performed with MPL and PHAD. These exhibited different phase transition temperatures at 33 °C and 57 °C, respectively. The onset temperature for the MPL phase transition is much lower and the range of MPL phase transition is much broader compared to PHAD (Fig. 2C). It is interesting to note that PHAD exhibited two phase transition temperatures with a major peak at 57 °C and minor peak at 63.6 °C.

3.3. FTIR analysis of the lipid a analogue phosphate groups

The phosphate groups are important functional groups for lipid A analogues and their presence is essential for endotoxin activity [26]. To determine the physical state of the phosphate groups for BECC438 and BECC470, we compared their infrared absorption spectra within the wavenumber range 1320–1180 cm^{-1}, which is the characteristic absorption of the negatively charged phosphate due to an antisymmetric stretching vibration [18,20]. For BECC438b and BECC470b, there is strong absorption peak at 1220 cm^{-1}, suggesting the phosphate groups are highly hydrated (Fig. 3A and B). In contrast, BECC438s, BECC470s, MPL, and PHAD do not have an absorption peak at 1220 cm^{-1}. Instead, they have is an additional band around 1260 cm^{-1}, which is more indicative that these lipid A analogues have phosphate groups that are poorly hydrated (Fig. 3).

3.4. UV–vis spectroscopy

To quantify the content of BECC438 or BECC470 in different formulations, we initially intended to develop an HPLC analysis method, however during method development we observed that BECC438b and BECC470b showed high UV absorbance (data not shown). Based on their structures, both BECC438 and BECC470 do not contain strong chromophores and should have weak UV absorbance. To investigate what is causing this absorbance in the UV range for the biologically derived BECC438b and BECC470b, UV–Vis spectra were obtained from 240 to 400 nm. As shown in Fig. 4, both BECC438b and BECC470b display strong UV absorbance from 240 to 280 nm with peak absorbance around 260 nm (Fig. 4A and B). In contrast, BECC438s, BECC470s, MPL, and PHAD exhibited much weaker absorbance in the same UV region, suggesting that the strong UV absorbance was a result of additional components present in the BECC438b and BECC470b preparations. The A_{260nm}/A_{280nm} ratios for BECC438b and BECC470b were close to 1.88, suggesting there could be nucleic acid contamination resulting from the preparation process [27]. For BECC438s, BECC470s, MPL, and PHAD, the ratio values of A_{260nm}/A_{280nm} were close to 1, which precluded the likelihood that there is nucleic acid present. To determine whether the unexpected UV absorbance in the BECC438b and BECC470b preparations was the result of nucleic acid being present, a dot blot assay using a RiboGreen assay was performed. Indeed, the dot blot assay with BECC438b and BECC470b showed a strong fluorescence signal while the synthetic BECCs, MPL and PHAD did not have any fluorescence signal (Fig. 4D). These findings confirmed that BECC438b and BECC470b contained a small amount of RNA (<4.5%). This small amount of nucleic acid contamination in the BECC438b and BECC470b preparations contributes most or all of the UV signal. For wavelengths above 300 nm, the optical density of synthetic BECCs was higher than their biological counterparts, perhaps due to the relatively larger size of the synthetic molecules, which do not contain any biosynthetic intermediates or congeners.

3.5. Analysis of aqueous formulations of the lipid a analogues

The hydrodynamic size of aqueous formulation of BECC438 or BECC470 was determined by dynamic light scattering (DLS) and

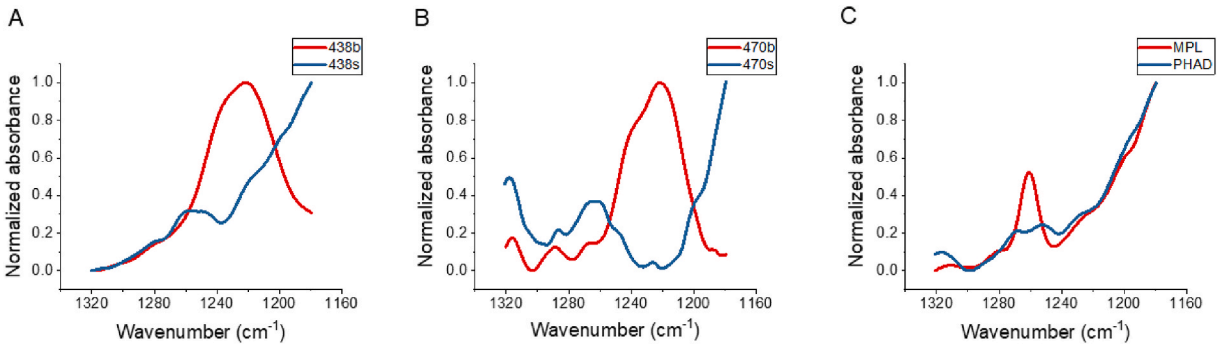

Fig. 3. FTIR analysis of the antisymmetric stretch of the phosphate groups. The FTIR spectra of BECC438b and BECC438s (A), BECC470b and BECC470s (B), and MPL and PHAD (C) are shown from 1320 to 1180 cm^{-1}.

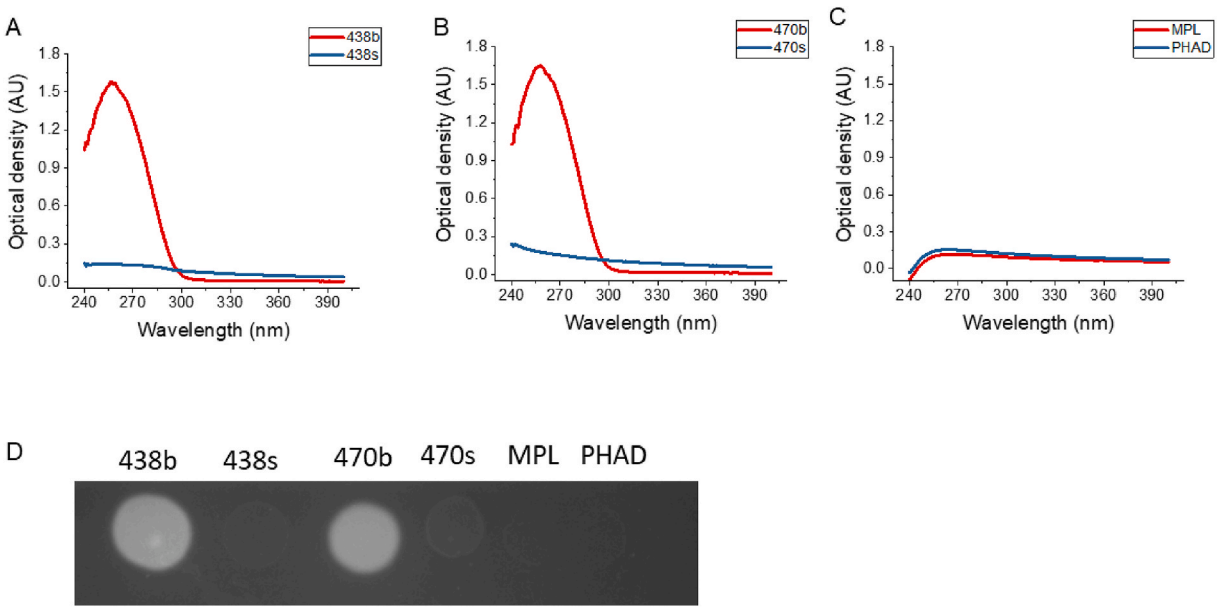

Fig. 4. UV–Vis absorbance spectra from 240 to 400 nm. Absorbance in the 260 nm range of the aqueous formulations suggests there may be RNA present in the biological BECC preparations. Panel A shows the absorbance spectra for BECC438b and BECC438s, panel B shows the spectra for BECC470b and BECC470s, and panel C shows the spectra for MPL and PHAD. Panel D shows the results of a dot blot assay of all six lipid A analogues after incubation with RiboGreen. The observed fluorescence for BECC438b and BECC470b suggests the presence of RNA. The original dot blot without cropping is shown in Suppl. Fig. S2.

these data are presented in Fig. 5 and Table 1. The average size of aqueous formulation for both the BECC438b or 470 b formulations was ~40 nm, whereas both BECC438s and BECC470s formulation exhibited a larger particle size that was near 80 nm. Whether this is due to the biological samples being a misture of congeners (with the structures shown in Suppl. Fig. S1 being the dominant structure) is not known. It is also possible that having mixed congeners in these biological samples influences the overall critical micelle

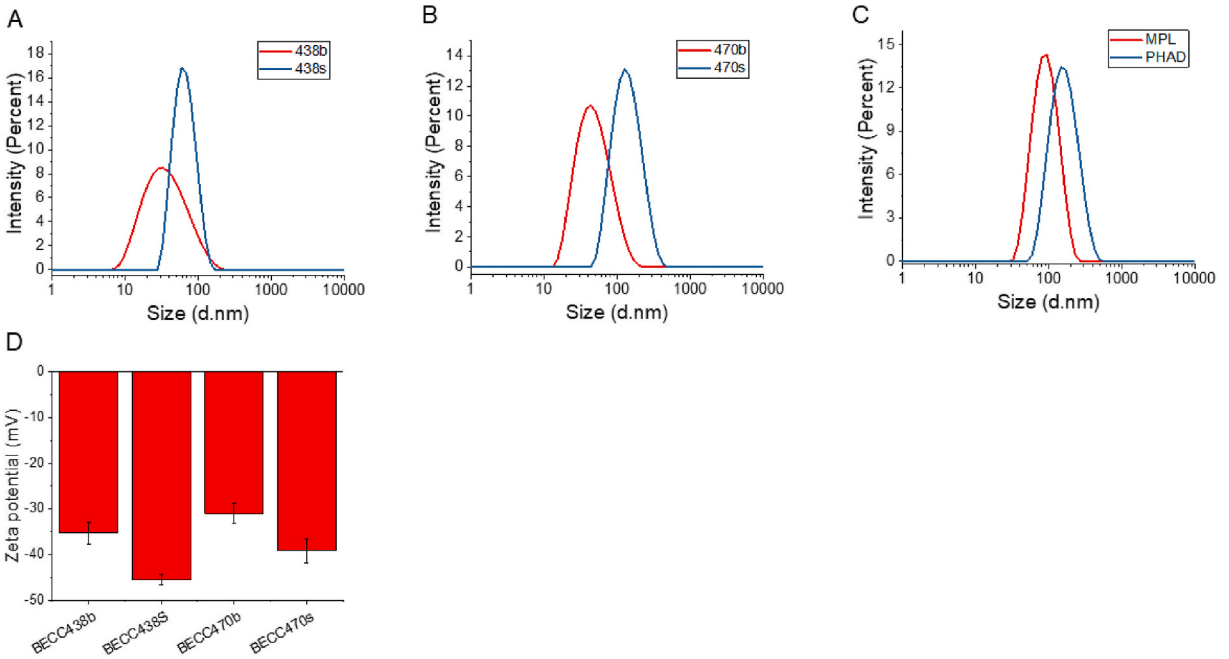

Fig. 5. The hydrodynamic properties of aqueous formulations determined by DLS and zeta potential assessment. Panel A shows the DLS data for BECC438b and BECC438s, panel B shows BECC470b and BECC470s, and panel C shows MPL and PHAD. Panel D shows the zeta potential values for the biological and synthetic forms of BECC438 and BECC470.

Table 1
The size of aqueous formulations for each of the lipid A analogues in aqueous solution is shown as determined using DLS.

Sample	Z-average (nm)	polydispersity
BECC438b	31.03 ± 0.61	0.286 ± 0.006
BECC438s	61.87 ± 0.38	0.114 ± 0.010
BECC470b	44.23 ± 2.08	0.253 ± 0.011
BECC470s	75.93 ± 0.55	0.202 ± 0.007
MPL	79.63 ± 1.69	0.194 ± 0.01
PHAD	143.0 ± 4.58	0.23 ± 0.03

concentration for the biological samples. For aqueous formulations of MPL and PHAD, the average particles sizes were 79 and 143 nm, respectively. The aqueous formulations for BECC438s and BECC470s have relatively narrow size distribution with smaller polydispersity (PDI) values compared to the biological BECC molecules. The zeta potentials for the aqueous formulations of BECC438 and BECC470 were also determined. The bis-phosphorylated BECC438 has a higher negative zeta potential compared with the mono-phosphosphorylated BECC470 as might be expected. The synthetic BECC438s and BECC470s have higher negative zeta values in comparison with their biological counterparts and the BECC438s was slightly more negative than BECC470 (Fig. 5D). Since the BECC438 contains two phosphate groups linked with the di-glucosamine backbone instead of the single phosphate group for BECC470, the higher negative zeta potential values for BECC438 were expected. The presence of a small amount of RNA in BECC438b and BECC470b may have resulted in their having a less negative zeta potential.

3.6. Detection of the lipid a analogues using the limulus amebocyte lysate (LAL) assay

The LAL assay is extensively used as a quantitative method for detecting endotoxin (lipopolysaccharide or LPS) produced by Gram-negative bacteria [24,28]. When activated by endotoxin, the LAL clotting enzyme releases an amide linked chromogenic *p*-nitroaniline (pNA) group from the modified peptide substrate, which is then measured spectroscopically. The LAL assay was used here to determine whether biological or synthetic BECC438 and BECC470 have similarly detected endotoxin levels when compared with MPL and PHAD. As shown in Fig. 6, BECC438b and BECC470b exhibited somewhat higher endotoxin levels (per mg) relative to MPL and PHAD. BECC438s had somewhat lower EU/mg than did BECC438b. Surprisingly, BECC470s showed negligible endotoxin levels that were almost at background level. The fact that BECC470b, prepared from a biological source, exhibited a much higher endotoxin level is most likely due to co-purifying congeners present within the sample. The endotoxin units for the biological BECC preparations and BECC438s were similar on an EU/mole basis to that observed for a commercial *E. coli* LPS (data not shown). How the LAL detection of these TLR4 agonists compares with their use in future vaccine formulations will be an important question to address in future studies. More importantly, because BECC470s is not readily detected by the LAL assay, questions arise with regard to its utility as a TLR4 agonist. This is despite the fact that both BECC438b and BECC470b have performed well as an adjuvant in animal trials [12–16].

3.7. Differential activation of NF-κB by the BECC TLR4 ligands

The ability of BECC438 and BECC470 to act as TLR4 ligands/agonists and to potentially cause inflammation was studied by NF-κB activation in mammalian cell lines. RAW-Blue cells, which stably expresses a secreted embryonic alkaline phosphatase (SEAP) gene inducible by NF-κB and AP-1 transcription factors, were stimulated with the ligands over a five-log concentration range for 18 h (Fig. 7A). SEAP activity was measured colorimetrically to determine the potential of the ligands to induce NF-κB, thereby indicating its TLR4 activation and potential inflammatory (and immunostimulatory) activity. *E. coli* BORT LPS was used as a positive control. Of the lipid A analogues tested here, BECC470b induced the highest level of NF-κB. Meanwhile, BECC470s elicited reduced levels of NF-κB activation, however, because this activation was readily seen, it does act as a TLR4 agonist despite not being detected by the LAL assay above. In contrast, THP-1-Dual cells (human) responded poorly to all ligands except the positive control (Fig. 7B). In parallel experiments, HEK-Blue cells overexpressing mouse (Fig. 7C) or human (Fig. 7D) TLR4 were also used for this study. Like RAW-Blue

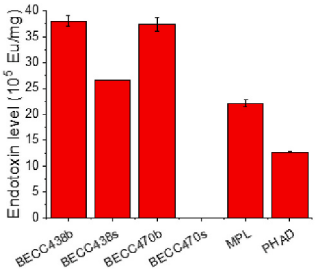

Fig. 6. The endotoxin units per mg of sample for aqueous formulations of BECC438 (b and s), BECC470 (b and s), MPL and PHAD are shown as determined using the Endosafe LAL assay.

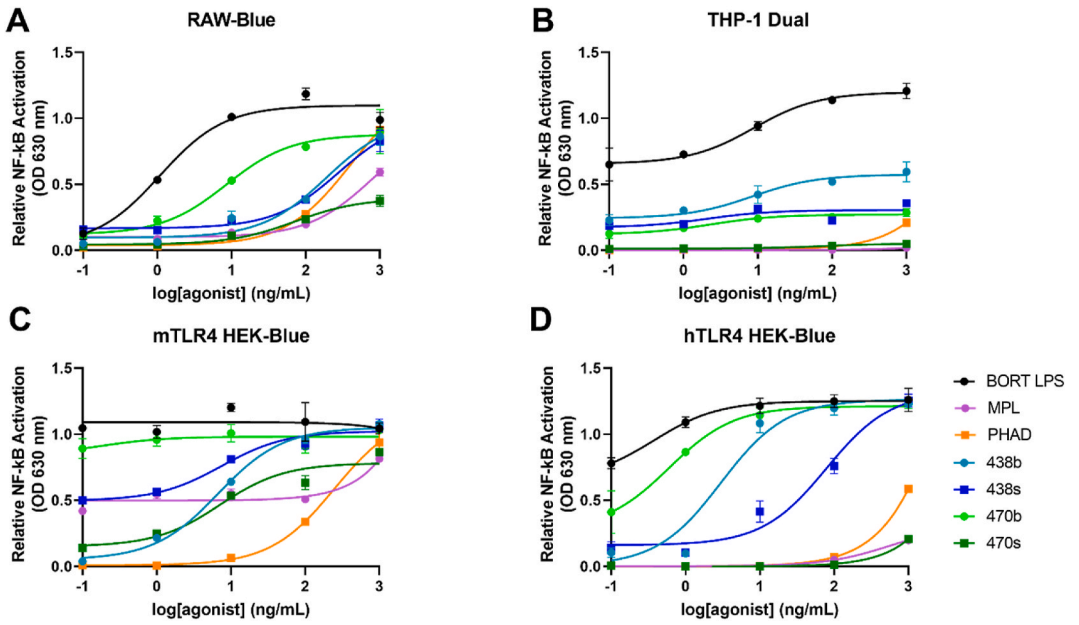

Fig. 7. Differential activation of NF-κB by TLR4 ligands. (A) RAW-Blue, (B), THP-1 Dual, (C) mTLR4 HEK-Blue and (D) hTLR4 HEK-Blue cell lines were stimulated with biological and synthetic BECC438 or BECC470, MPL or PHAD over a five-log dilution series. SEAP activity was measured using Quanti-Blue at an optical density of 620 nm. When RAW-Dual cells with TLR4 knocked out were tested as a negative control, no detectable FN-κB activity was seen for any of these lipid A analogues or for *E. coli* BORT LPS (not shown). Mean results ± SD are graphed with a sigmoidal nonlinear regression of best fit.

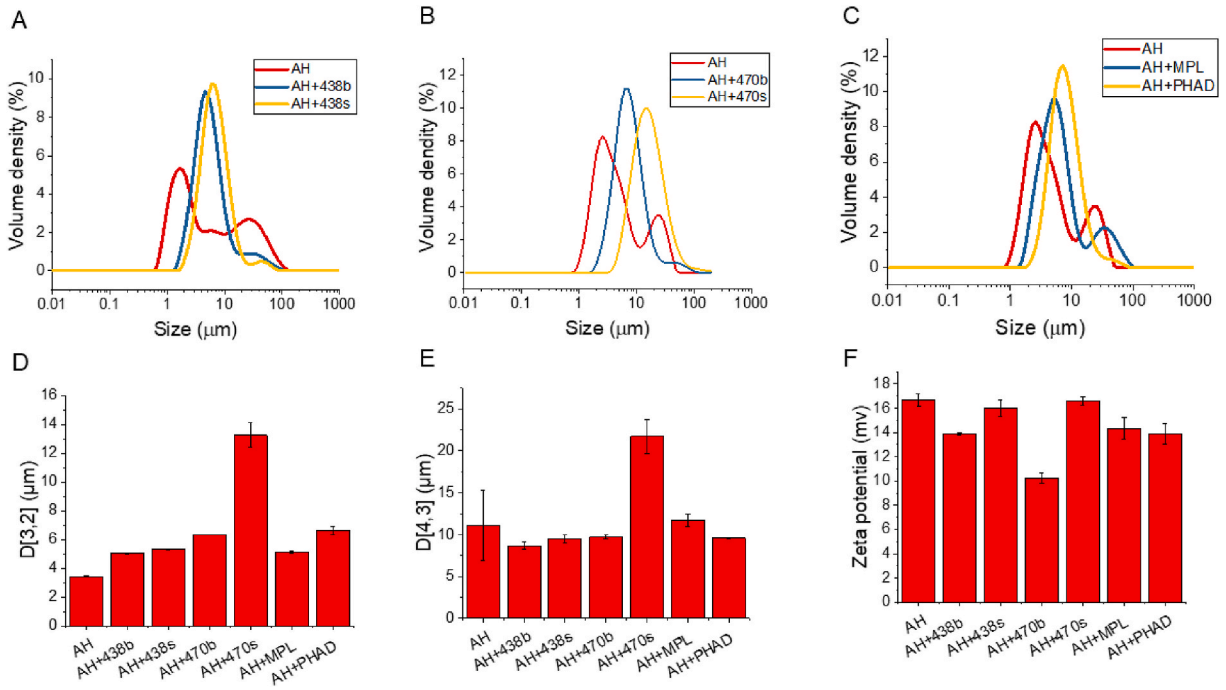

Fig. 8. Particle characterization of Alhydrogel (AH) formulations as a function of lipid A binding is shown. (A) The size distribution of AH is shown alone and after adsorption of BECC438b and BECC438s. (B) The size distribution of AH is shown alone and after adsorption of BECC470b and BECC470s. (C) The size distribution of AH is shown alone and after adsorption of MPL and PHAD. (D) The surface area moment mean D [3,2] is shown for each of the AH formulations. (E) The volume moment mean D [4,3] of AH is shown for each of the formulations. (F) The zeta surface potential of AH for each of the formulations is also shown.

(expressing only endogenous mTLR4), mTLR4 over-expressing cells responded at the highest level to BECC470b stimulation. In this case, however, PHAD stimulated NF-κB activation the poorest. In the case of hTLR4 over-expressing HEK-Blue cells, BECC470b afforded the highest stimulation whereas, BECC470s and MPL had the lowest stimulation capability. Ultimately, the synthetic BECC molecules had lower NF-κB driven responses, as compared to biological forms, except in the case of mTLR4 HEK-Blue, where BECC438s had a slightly higher stimulation potential than BECC438b.

3.8. Characterization after BECC438 and BECC470 adsorbed to alhydrogel (AH)

We next examined the efficiency of adsorption of BECC438 or BECC470 (both biological and synthetic) in parallel with MPL and PHAD onto Alhydrogen (AH). We then compared the effect of adsorption to AH on the properties of the particles for all these lipid A analogues. This was done to demonstrate the potential use of these BECC molecules as biosimilars in GSK's AS04 adjuvant system (10:1 mass ratio of AH with MPL, respectively). We first determined how readily BECC438, BECC470, MPL and PHAD was adsorbed to Alhydrogel at a 10:1 mass ratio. For both BECC438b, BECC438s and BECC470b, 100% of the lipid A analogues was adsorbed to the AH as determined by their complete removal from the supernatant fractions according to the LAL detection assay (data not shown). This was also the case for MPL and PHAD. However, because the LAL assay does not detect BECC470s, its adsorption efficiency could not be easily determined in this way, however, the parallel data presented below strongly suggest that BECC470s interacts with AH as efficiently as the other lipid A analogues.

The effect of each lipid A analogue on the size and zeta potential of the formulated AH particles was next determined. AH has a relatively broad size distribution ranging from 1 to 100 μm (Fig. 8). In all cases, adsorption of the lipid A analogue led to a consolidation of AH particles to a dominant intermediate size (Fig. 8 A-C). Also worth noting, in all cases, the synthetic lipid A analogue gave rise to a final larger AH particle size than did its biological counterpart (Fig. 8 A-C). Because BECC470s adsorption to AH resulted in the same changes in AH particle size and size distribution, it appears safe to assume it is binding with an efficiency that compares favorably with the other molecules.

AH's surface area moment mean D [3,2], which is most sensitive to the presence of the fine particles in the size distribution, is smaller at 3.16 μm than AH adsorbed with any of the lipid A analogues (Fig. 8D). On the other hand, AH's volume moment mean D [4,3], which is most sensitive to the presence of large particles in the size distribution, is similar to AH with adsorbed BECC438b, BECC438s, BECC470b, MPL or PHAD (Fig. 8E). For BECC438, the particle size of AH with the adsorbed biological or synthetic molecule is similar to AH with adsorbed BECC470b, and these values are all much smaller than the D [3,2] and D [4,3] for BECC470s adsorbed to the AH. The reason for this variation with BECC470s is not yet clear. The change of zeta potential for AH after BECC438 or BECC470 adsorption was also evaluated. AH at pH 7 is positively charged at 16.7. After the addition of BECC438 or BECC470, a decrease in the positive zeta potential of AH is observed (Fig. 8F), but AH with BECC438b or BECC470b decreased more compared to AH with adsorbed BECC438s or BECC470s (Fig. 8F). The latter observation may be due to the presence of BECC congeners or RNA impurities.

3.9. Emulsion formulation with BECC438 and BECC470

Lastly, we evaluated whether BECC438 or BECC470 could be co-formulated with an oil-in-water emulsion termed Medimmune emulsion or ME. This formulation is an approximate biosimilar of GSK's squalene-containing AS03 adjuvant lacking the α-tocopherol. BECC438 and BECC470 did not appear to incorporate efficiently into the ME particle through simple admixing since the majority of the endotoxin units remained in the aqueous phase ad determined using the LAL assay (data not shown). It should be noted, however, that this would not determine whether the BECC molecules were associating loosely with these particles. In contrast, most of BECC438 and BECC470 (biological or synthetic) does appear to be incorporated into the ME emulsion particles when co-formulated with ME (i.e. when the lipid A analogue is added during the emulsion preparation). In this case, the lipophilic acyl chains of the BECC438 and

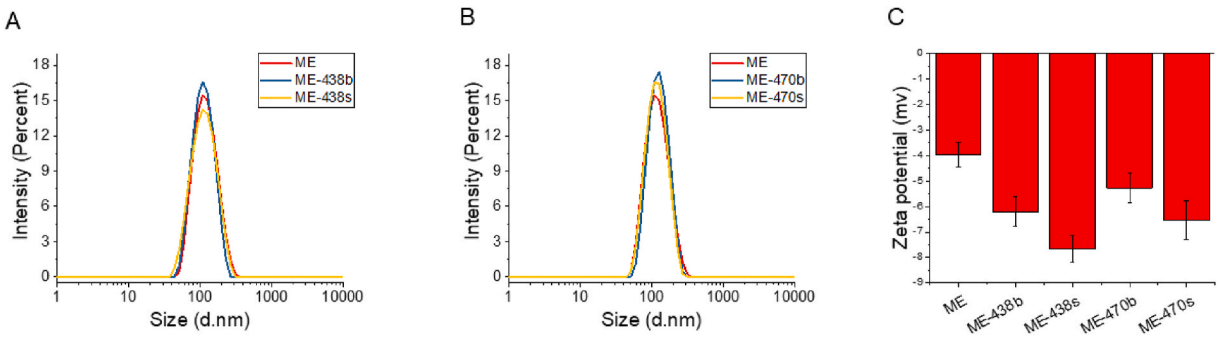

Fig. 9. Particle characterization of ME and ME-lipid A co-formulations. (A) The size distribution of ME co-formulated with BECC438b and BECC438s does not appear to change substantially. (B) Likewise, the size distribution of ME co-formulated with BECC470b and BECC470s remains rather constant. (C) The zeta potentials for ME and the ME-lipid A co-formulations are different due to the negative charge contributes by the lipid A analogues.

BECC470 would be expected to extend into the oil phase of the droplets while disaccharide and phosphate groups would be expected to interact with the aqueous phase. Indeed, based on LAL assay, more that 98% of the BECC438 or BECC470 appears to be incorporated into ME nanoparticles as they were excluded from detection in the aqueous phase by the LAL assay (data not shown). To further assess whether the BECC molecules were fully incorporated into the emulsion particles, zeta potential measurements were performed for the co-formulated ME-BECC emulsions and the ME emulsion alone (Fig. 9). The increase in negative zeta potential in the co-formulated ME-BECC indicated incorporation of the BECC438 or BECC470 into the particles with the change in charge most likely due to the newly introduced surface phosphate groups. Interestingly, the particle size of ME did not noticeably change in the presence of the BECC molecules after co-formulation (Fig. 9 and Table 2).

4. Discussion

We conducted a comprehensive physicochemical characterization on two novel lipid A-based TLR4 agonists, BECC438 and BECC470, in their biologically derived and chemically synthesized forms. The synthetic BECC438s and BECC470s have a high degree of purity and homogeneity based on mass spectrometric analyses and HPLC analyses, while biological BECC438b and BECC470b contain a small amount of co-purifying nucleic acid (<5%). BECC438b has been shown to possess potent adjuvant activity in experimental vaccines against *Y. pestis* (plague) and *Pseudomonas aeruginosa* (pulmonary infections) [12,13]. Likewise, BECC470b demonstrated strong adjuvant activity in vaccines that could protect against influenza A and SARS-CoV-2 [15,16]. By understanding the biophysical properties of these adjuvants and their more highly purified synthetic versions, the use of these TLR4 agonists in novel vaccine formulations will expand the existing arsenal of safe and effective vaccines for protecting human health. Furthermore, the two synthetic molecules (BECC438s and BECC470s) represent adjuvant candidates that are structurally defined, and which can be prepared with no lot-to-lot variation (Suppl. Fig. S1) as occurs for biological preparations such as MPL.

The phase transition experiments using FTIR and DSC show that there is an altered packing pattern of the acyl chains for BECC438b and BECC470b, as compared with their synthetic counterparts. Neither BECC438b nor BECC470b demonstrated a detectable phase transition in these experiments. In contrast, clearly visible phase transitions were seen for BECC438s and BECC470s with both having a similar transition temperature (~40 °C). It is perhaps not surprising that BECC438s and BECC470s have nearly identical phase transition temperatures since they possess the same hexa-acyl chain patterns and the additional phosphate group of BECC438s would not be expected to greatly impact acyl chain packing. Furthermore, the FTIR peak position at 2854 cm^{-1} at 25 °C for BECC438b and BECC470b indicate that the hexa-acyl chains are in a disordered liquid-crystalline phase even at low temperatures. This may be due to the heterogeneity in the BECC438b and BECC470b preparations caused by the coextraction and purification of alternate congeners, although the major product for each extraction is BECC438b and BECC470b, respectively. The likely existence of molecules with penta-acyl or tetra-acyl chains for the biological BECC molecules would likely disrupt the tight packing interactions among hexa-acyl chains. Although MPL displayed a detectable phase transition near 36 °C, the peak position at 2851.75 cm^{-1} indicates that the hexa-acyl chains are in a mixed state with some in an ordered gel phase and others in a less ordered liquid-crystalline phase. It is difficult to overcome the inherent heterogeneity problem for lipid A analogues purified from biological sources, which makes their synthetic counterparts attractive for future well-defined vaccine formulations.

The phase transition temperatures for these lipid A analogues as determined by FTIR were confirmed by DSC. It is interesting, however, that PHAD exhibited a higher phase transition temperature than did BECC438s and BECC470s, since the phase transition temperature is dependent on the number of acyl chains and the length of acyl chains. For PHAD, BECC438s, and BECC470s, four primary acyl chains of 14 carbons are bound to the disaccharide backbone at the two amino and two hydroxyl groups are bound at the 2-, 2′ and 3-, 3′- positions. In PHAD, two secondary acyl groups (12 and 14 carbons) form 3-acyloxyacyl structures in D-gluocosamine II (GlcN(II)) generating an asymmetrical acylation pattern of the (4 + 2)-type, where GlcN(I) is linked to two acyl chains while GlcN(II) is linked to four acyl chains. BECC438s and BECC470s have a symmetrical (3 + 3)-type acylation pattern, and one secondary acyl group with 16 carbons form 3-acyloxyacyl structure in GlcN(I) and GlcN(II). The secondary acyl group in GlcN(II) contains one double bond. It appears that the acylation pattern and the double bond in the acyl chain may have an impact on the packing density of the hydrocarbon chains, which results in lower phase transition temperatures for BECC438s and BECC470s when compared to PHAD.

The FTIR measurement of the vibrational bands of the phosphate groups in these lipid A analogues reveals clear differences between the BECC438b and BECC470b preparations and their synthetic counterparts. The phosphate groups in BECC438b and BECC470b exhibit a high degree of hydration, which could perhaps be a result of the small amount of nucleic acid impurities in these preparations. Nevertheless, the absence of a band component at 1257 cm^{-1} suggests that the phosphate groups in BECC438b and BECC470b are fully hydrated. For BECC438s and BECC470s, the phosphate groups are poorly hydrated and may be buried in the

Table 2
Size of oil-in-water emulsion ME and ME-lipid A analogue coformulations were determined by dynamic light scattering.

Sample	Z-average (nm)	polydispersity
ME	114.0 ± 2.64	0.154 ± 0.012
ME-438 b	104.2 ± 1.26	0.080 ± 0.013
ME-438s	102.7 ± 0.57	0.123 ± 0.029
ME-470 b	111.2 ± 2.06	0.128 ± 0.014
ME-470s	106.8 ± 1.50	0.116 ± 0.018

backbone close to the hydrophobic regions of neighboring molecules within their micellar assemblies.

In aqueous formulations, the z-average values of BECC438b and BECC470b are smaller than those of their synthetic counterparts. This is also the case for biologically derived MPL versus synthetic PHAD and could be due to differences in their supramolecular structures. Although the dominant species in the biologically derived BECC438b and BECC470b preparations contain hexa-acyl chains, the occurrence of penta-acyl and tetra-acyl forms cannot be excluded since. The relatively higher polydispersity of BECC438*b* and BECC470*b* would then also be expected to result from their overall structural heterogeneity. With respect to zeta potential values, BECC438 had larger negative values compared with BECC470, which is consistent with BECC438 containing two phosphate groups instead of one as is the case for BECC470. It is worth noting that the biologically derived BECC molecules exhibited lower negative values in comparison with their synthetic counterparts, which again may be due to the small amount of nucleic acid impurities present in BECC438b and BECC470b.

The BECC platform was designed to identify lipid A analogues that had reduced toxicity while retaining adjuvant potential. That said, it has been reported that maximal lipid A toxicity is achieved with bis-phosphorylated, hexa-acylated lipid A species [29]. Lipid A analogues that are structurally different from this often demonstrate a significant reduction in endotoxic activity [30]. It has been confirmed that acyl chains 14 carbons in length provide greater potency, but this toxicity declines rapidly with chain lengths less than 10 or greater than 16 [31,32]. Two phosphate groups in lipid An also are a contributing factor affecting the endotoxic activity [26]. Deletion of either phosphate reduces toxicity by ~100 fold [33,34]. The endotoxin potential of lipid A is often measured using the Limulus amoebocyte lysis (LAL) assay, which is affected by both the number and the length of acyl chains and the presence of phosphate groups. It was surprising to observe that BECC470b containing a single phosphate group has higher endotoxin levels as measured by the LAL assay than the bis-phosphorylated BECC438b. Then, in complete contrast, BECC470s exhibited negligible to no endotoxin activity as measured using the LAL assay. Nevertheless, all of these lipid A analogues, including BECC470s, demonstrated TLR4 agonist activity as determined using cell-based assays. This perhaps bodes well for including the synthetic BECC470s in vaccine formulations since it should not interfere with monitoring the "endotoxicity" of formulations containing this adjuvant according to these findings.

There is an established connection between the biological activity of lipid A and their supramolecular structures. Lipid A samples with conical molecular conformations in their nonlamellar structures tend to be highly active, while lipid A samples with cylindrical molecular conformations in their lamellar structures tend to be inactive. Those with partly conical molecular conformations in mixed lamellar/cubic structures then have intermediate activities. Without small-angle X-ray diffraction, we cannot determine the three-dimensional organization of lipid A samples in aqueous suspensions but based on the endotoxin units per mg exhibited by these lipid A samples, it may be reasonable to suggest that most of the BECC470s is present in the cylindrical molecular conformation in their lamellar structures while most of the BECC470b assumes the cylindrical molecular conformation in their nonlamellar structures. Future studies on the micellar assembly of these different lipid A analogues may shed light on the fact that the LAL assay signal for BECC470s is absent while it still has TLR4 agonist potential in cell-based assays.

Due to the lipophilic nature of the acyl chains in lipid A-like TLR4 agonists, they do not readily solubilize in aqueous solutions and instead can form undefined aggregates that can decrease their immunostimulatory effect. Without proper formulation, these TLR4 agonists may have reduced or limited efficacy and these agonists may fail to induce the required vaccine-induced responses [6,35]. This is why these molecules are often included in formulations with other immunostimulatory molecules such as Alhydrogel (AH) or squalene. Similar to MPL and PHAD, BECC438 and BECC470 (biological or synthetic) can be co-formulated with AH with almost 100% adsorption efficiency at neutral pH, which is facilitated by electrostatic interactions between negatively charged TLR4 agonists with the positively charged aluminum gels [36,37]. Other mechanisms, such as ligand exchange and hydrophobic interactions, may also play important roles in the binding [36]. The change of size distribution of AH after the adsorption of lipid A and these analogues may be a function of the phosphate groups, which results in a decrease in the zeta potential for the particle. Oil-in-water emulsions represent another important formulation platform for the delivery of TLR4 agonists [38–40]. Oil-in-water emulsions that include squalene have a proven safety profile and are approved for use as human vaccine adjuvants [41]. BECC438 and BECC470 can be co-formulated with ME emulsion with almost 100% incorporation efficiency. LAL analysis of aqueous extractions of ME containing BECC438 or BECC470 found that the adjuvants were each associated with the oil phase with co-formulation. This was also confirmed by zeta potential measurements, which indicated that the anionic lipid A analogues were present at the oil/water interface, giving rise to a more negatively charged particle. The combination of TLR4 agonists with previously approved adjuvants, including AH and oil-in-water emulsions, can lead to synergistic enhancement of the resulting immune response and allow for vaccine antigen dose sparing and vaccine dose sparing [6,12,15].

The binding of lipid A to TLR4/MD2 complexes activates two different intracellular signaling pathways, MyD88 and TRIF [42,43]. The MyD88 pathway activates mitogen-activated protein kinase (MAPK) and nuclear factor-κb (NF-κb) dependent pro-inflammatory responses, while the TRIF pathway activates kinases responsible for type I interferon responses [44]. It has been reported that MPL preferentially activates the TLR4-TRIF-based signaling pathway but not the TLR4-MyD88 pathway [45]. It has also been reported that BECC438b and BECC470b induced a lower pro-inflammatory response with reporter cell lines in comparison with *E. coli* LPS [11,12]. Furthermore, cytokine secretion levels of TNF-α and IL-8 during *in vitro* experiments were comparable to those induced by PHAD [11,12]. It is highly anticipated that BECC438s and BECC470s will behave like their less pure and less homogeneous biological counterparts by preferentially activating TLR4-TRIF-based signaling pathway. This would be consistent with synthetic PHAD, which is a less potent endotoxin than the biologically derived MPL [46]. Ongoing preliminary studies in mice suggest that this will indeed be the case (data not shown). Nevertheless, it will be interesting to determine whether BECC438s and BECC470s maintain the strong adjuvant potential that is inherent to their biological counterparts.

5. Conclusion

With an urgent need for new, safe, and potent adjuvants for vaccine development, this work provided detailed physiochemical characterization of two new TLR4 agonists, BECC438 and BECC470. In this study, the synthetic versions of each lipid A analogue exhibited distinct physicochemical properties relative to their biological counterparts, including phase transition temperature and phosphate conformation. All of these lipid A molecules can be formulated into different forms, especially in combination with other adjuvants such as AH or oil-in-water emulsions. Synthetic lipid A molecules have advantages over bacterially derived products in that they are chemically defined, highly purified products with the ability to be generated with little to no variation between preparations. Furthermore, scale up of chemical synthesis will provide a reduced cost, thus reducing the price of vaccines containing them. BECC438s and BECC470s thus have great potential as safe and highly potent adjuvants for human vaccines.

Author contribution statement

Gang Hu: Performed the experiments; Analyzed and interpreted the data; Wrote the paper.
David J Varisco: Performed the experiments; Contributed reagents, materials, analysis tools or data.
Sayan Das: Performed the experiments; Analyzed and interpreted the data.
C Russell Middaugh: Conceived and designed the experiments; Analyzed and interpreted the data.
Francesca Gardner and Wendy L Picking: Contributed reagents, materials, analysis tools or data.
Robert K Ernst: Conceived and designed the experiments; Contributed reagents, materials, analysis tools or data.
William Picking: Conceived and designed the experiments; Analyzed and interpreted the data; Wrote the paper.

Data availability statement

Data will be made available on request.

Declaration of competing interest

The authors declare that they have no known competing financial interests or personal relationships that could have appeared to influence the work reported in this paper

Acknowledgements

This project has been funded in whole with Federal funds from the National Institutes of Health, under Contract No. and HHSN272201800043C to RKE. The content of this publication does not necessarily reflect the views or policies of the Department of Health and Human Services, nor does mention of trade names, commercial products, or organizations imply endorsement by the U.S. Government.

Appendix A. Supplementary data

Supplementary data to this article can be found online at https://doi.org/10.1016/j.heliyon.2023.e18119.

References

[1] A.M. Didierlaurent, S. Morel, L. Lockman, S.L. Giannini, M. Bisteau, H. Carlsen, A. Kielland, O. Vosters, N. Vanderheyde, F. Schiavetti, D. Larocque, M. Van Mechelen, N. Garçon, AS04, an aluminum salt- and TLR4 agonist-based adjuvant system, induces a transient localized innate immune response leading to enhanced adaptive immunity, J. Immunol. 183 (10) (2009) 6186–6197.
[2] J.T. Evans, C.W. Cluff, D.A. Johnson, M.J. Lacy, D.H. Persing, J.R. Baldridge, Enhancement of antigen-specific immunity via the TLR4 ligands MPL adjuvant and Ribi.529, Expert Rev. Vaccines 2 (2) (2003) 219–229.
[3] N. Garçon, M. Van Mechelen, Recent clinical experience with vaccines using MPL- and QS-21-containing adjuvant systems, Expert Rev. Vaccines 10 (4) (2011) 471–486.
[4] T.F. Schwarz, L.M. Huang, D.M. Medina, A. Valencia, T.Y. Lin, U. Behre, G. Catteau, F. Thomas, D. Descamps, Four-year follow-up of the immunogenicity and safety of the HPV-16/18 AS04-adjuvanted vaccine when administered to adolescent girls aged 10-14 years, J. Adolesc. Health 50 (2) (2012) 187–194.
[5] C.R. Casella, T.C. Mitchell, Putting endotoxin to work for us: monophosphoryl lipid A as a safe and effective vaccine adjuvant, Cell. Mol. Life Sci. 65 (20) (2008) 3231–3240.
[6] G.C. Ireton, S.G. Reed, Adjuvants containing natural and synthetic Toll-like receptor 4 ligands, Expert Rev. Vaccines 12 (7) (2013) 793–807.
[7] J. Falloon, F. Ji, C. Curtis, S. Bart, E. Sheldon, D. Krieger, F. Dubovsky, S. Lambert, T. Takas, T. Villafana, M.T. Esser, A phase 1a, first-in-human, randomized study of a respiratory syncytial virus F protein vaccine with and without a toll-like receptor-4 agonist and stable emulsion adjuvant, Vaccine 34 (25) (2016) 2847–2854.
[8] D.S. Heeke, R. Lin, E. Rao, J.C. Woo, M.P. McCarthy, J.D. Marshall, Identification of GLA/SE as an effective adjuvant for the induction of robust humoral and cell-mediated immune responses to EBV-gp350 in mice and rabbits, Vaccine 34 (23) (2016) 2562–2569.
[9] A. Pantel, C. Cheong, D. Dandamudi, E. Shrestha, S. Mehandru, L. Brane, D. Ruane, A. Teixeira, L. Bozzacco, R.M. Steinman, M.P. Longhi, A new synthetic TLR4 agonist, GLA, allows dendritic cells targeted with antigen to elicit Th1 T-cell immunity in vivo, Eur. J. Immunol. 42 (1) (2012) 101–109.

[10] M. Santini-Oliveira, R.N. Coler, J. Parra, V. Veloso, L. Jayashankar, P.M. Pinto, M.A. Ciol, R. Bergquist, S.G. Reed, M. Tendler, Schistosomiasis vaccine candidate Sm14/GLA-SE: phase 1 safety and immunogenicity clinical trial in healthy, male adults, Vaccine 34 (4) (2016) 586–594.
[11] K.A. Gregg, E. Harberts, F.M. Gardner, M.R. Pelletier, C. Cayatte, L. Yu, M.P. McCarthy, J.D. Marshall, R.K. Ernst, Rationally designed TLR4 ligands for vaccine adjuvant discovery, mBio 8 (3) (2017).
[12] K.A. Gregg, E. Harberts, F.M. Gardner, M.R. Pelletier, C. Cayatte, L. Yu, M.P. McCarthy, J.D. Marshall, R.K. Ernst, A lipid A-based TLR4 mimetic effectively adjuvants a Yersinia pestis rF-V1 subunit vaccine in a murine challenge model, Vaccine 36 (28) (2018) 4023–4031.
[13] D.R. Howlader, S. Das, T. Lu, G. Hu, D.J. Varisco, Z.K. Dietz, S.P. Walton, S.S.K. Ratnakaram, F.M. Gardner, R.K. Ernst, W.D. Picking, W.L. Picking, Effect of two unique nanoparticle formulations on the efficacy of a broadly protective vaccine against Pseudomonas aeruginosa, Front. Pharmacol. 12 (2021), 706157.
[14] A. Zacharia, E. Harberts, S.M. Valencia, B. Myers, C. Sanders, A. Jain, N.R. Larson, C.R. Middaugh, W.D. Picking, S. Difilippantonio, R. Kirnbauer, R.B. Roden, L. A. Pinto, R.H. Shoemaker, R.K. Ernst, J.D. Marshall, Optimization of RG1-VLP vaccine performance in mice with novel TLR4 agonists, Vaccine 39 (2) (2021) 292–302.
[15] R.E. Haupt, E.M. Harberts, R.J. Kitz, S. Strohmeier, F. Krammer, R.K. Ernst, M.B. Frieman, Novel TLR4 adjuvant elicits protection against homologous and heterologous Influenza A infection, Vaccine 39 (36) (2021) 5205–5213.
[16] T.Y. Wong, K.S. Lee, B.P. Russ, A.M. Horspool, J. Kang, M.T. Winters, M. Allison Wolf, N.A. Rader, O.A. Miller, M. Shiflett, J. Izac, D. Varisco, E. Sen-Kilic, C. Cunningham, M. Cooper, H.A. Cyphert, M. Barbier, I. Martinez, J.R. Bevere, R.K. Ernst, F.H. Damron, Intranasal administration of BReC-CoV-2 COVID-19 vaccine protects K18-hACE2 mice against lethal SARS-CoV-2 challenge, NPJ Vaccines 7 (1) (2022) 36.
[17] J.R. Baldridge, R.T. Crane, Monophosphoryl lipid A (MPL) formulations for the next generation of vaccines, Methods 19 (1) (1999) 103–107.
[18] S. Fukuoka, K. Brandenburg, M. Müller, B. Lindner, M.H. Koch, U. Seydel, Physico-chemical analysis of lipid A fractions of lipopolysaccharide from Erwinia carotovora in relation to bioactivity, Biochim. Biophys. Acta 1510 (1–2) (2001) 185–197.
[19] R. Toman, P. Garidel, J. Andrä, K. Slaba, A. Hussein, M.H. Koch, K. Brandenburg, Physicochemical characterization of the endotoxins from Coxiella burnetii strain Priscilla in relation to their bioactivities, BMC Biochem. 5 (2004) 1.
[20] K. Brandenburg, S. Kusumoto, U. Seydel, Conformational studies of synthetic lipid A analogues and partial structures by infrared spectroscopy, Biochim. Biophys. Acta 1329 (1) (1997) 183–201.
[21] R.N. Lewis, R.N. McElhaney, Membrane lipid phase transitions and phase organization studied by Fourier transform infrared spectroscopy, Biochim. Biophys. Acta 1828 (10) (2013) 2347–2358.
[22] E. Franco, V. Garcia-Recio, P. Jiménez, M. Garrosa, T. Girbés, M. Cordoba-Diaz, D. Cordoba-Diaz, Endotoxins from a pharmacopoeial point of view, Toxins 10 (8) (2018).
[23] J. Levin, F.B. Bang, The role of endotoxin in the extracellular coagulation of limulus blood, Bull. Johns Hopkins Hosp. 115 (1964) 265–274.
[24] T. Nakamura, T. Morita, S. Iwanaga, Lipopolysaccharide-sensitive serine-protease zymogen (factor C) found in Limulus hemocytes. Isolation and characterization, Eur. J. Biochem. 154 (3) (1986) 511–521.
[25] V. Iyer, C. Cayatte, J.D. Marshall, J. Sun, K. Schneider-Ohrum, S.K. Maynard, G.M. Rajani, A.S. Bennett, R.L. Remmele Jr., S.M. Bishop, M.P. McCarthy, B. K. Muralidhara, Feasibility of freeze-drying oil-in-water emulsion adjuvants and subunit proteins to enable single-vial vaccine drug products, J. Pharmaceut. Sci. 106 (6) (2017) 1490–1498.
[26] E.T. Rietschel, T. Kirikae, F.U. Schade, U. Mamat, G. Schmidt, H. Loppnow, A.J. Ulmer, U. Zähringer, U. Seydel, F. Di Padova, et al., Bacterial endotoxin: molecular relationships of structure to activity and function, Faseb. J. 8 (2) (1994) 217–225.
[27] J.A. Glasel, Validity of nucleic acid purities monitored by 260nm/280nm absorbance ratios, Biotechniques 18 (1) (1995) 62–63.
[28] U. Seydel, L. Hawkins, A.B. Schromm, H. Heine, O. Scheel, M.H. Koch, K. Brandenburg, The generalized endotoxic principle, Eur. J. Immunol. 33 (6) (2003) 1586–1592.
[29] C.R. Raetz, C. Whitfield, Lipopolysaccharide endotoxins, Annu. Rev. Biochem. 71 (2002) 635–700.
[30] C. Alexander, E.T. Rietschel, Bacterial lipopolysaccharides and innate immunity, J. Endotoxin Res. 7 (3) (2001) 167–202.
[31] D.A. Johnson, D.S. Keegan, C.G. Sowell, M.T. Livesay, C.L. Johnson, L.M. Taubner, A. Harris, K.R. Myers, J.D. Thompson, G.L. Gustafson, M.J. Rhodes, J. T. Ulrich, J.R. Ward, Y.M. Yorgensen, J.L. Cantrell, V.G. Brookshire, 3-O-Desacyl monophosphoryl lipid A derivatives: synthesis and immunostimulant activities, J. Med. Chem. 42 (22) (1999) 4640–4649.
[32] A.G. Stöver, J. Da Silva Correia, J.T. Evans, C.W. Cluff, M.W. Elliott, E.W. Jeffery, D.A. Johnson, M.J. Lacy, J.R. Baldridge, P. Probst, R.J. Ulevitch, D.H. Persing, R.M. Hershberg, Structure-activity relationship of synthetic toll-like receptor 4 agonists, J. Biol. Chem. 279 (6) (2004) 4440–4449.
[33] C. Cekic, C.R. Casella, C.A. Eaves, A. Matsuzawa, H. Ichijo, T.C. Mitchell, Selective activation of the p38 MAPK pathway by synthetic monophosphoryl lipid A, J. Biol. Chem. 284 (46) (2009) 31982–31991.
[34] M. Tsujimoto, S. Kotani, T. Okunaga, T. Kubo, H. Takada, T. Kubo, T. Shiba, S. Kusumoto, T. Takahashi, Y. Goto, et al., Enhancement of humoral immune responses against viral vaccines by a non-pyrogenic 6-O-acylmuramyldipeptide and synthetic low toxicity analogues of lipid, A. Vaccine 7 (1) (1989) 39–48.
[35] M. Mueller, B. Lindner, S. Kusumoto, K. Fukase, A.B. Schromm, U. Seydel, Aggregates are the biologically active units of endotoxin, J. Biol. Chem. 279 (25) (2004) 26307–26313.
[36] C.R. Alving, G.R. Matyas, Design and Selection of Vaccine Adjuvants: Principles and Practice. The Grand Challenge for the Future, Springer, 2005, pp. 99–118.
[37] D. Zhu, S. Huang, E. Gebregeorgis, H. McClellan, W. Dai, L. Miller, A. Saul, Development of a direct alhydrogel formulation immunoassay (DAFIA), J. Immunol. Methods 344 (1) (2009) 73–78.
[38] R.C. Anderson, C.B. Fox, T.S. Dutill, N. Shaverdian, T.L. Evers, G.R. Poshusta, J. Chesko, R.N. Coler, M. Friede, S.G. Reed, T.S. Vedvick, Physicochemical characterization and biological activity of synthetic TLR4 agonist formulations, Colloids Surf. B Biointerfaces 75 (1) (2010) 123–132.
[39] R.N. Coler, S. Bertholet, M. Moutaftsi, J.A. Guderian, H.P. Windish, S.L. Baldwin, E.M. Laughlin, M.S. Duthie, C.B. Fox, D. Carter, M. Friede, T.S. Vedvick, S. G. Reed, Development and characterization of synthetic glucopyranosyl lipid adjuvant system as a vaccine adjuvant, PLoS One 6 (1) (2011), e16333.
[40] M. Singh, J. Kazzaz, M. Ugozzoli, B. Baudner, M. Pizza, M. Giuliani, L.D. Hawkins, G. Otten, D.T. O'Hagan, MF59 oil-in-water emulsion in combination with a synthetic TLR4 agonist (E6020) is a potent adjuvant for a combination Meningococcus vaccine, Hum. Vaccines Immunother. 8 (4) (2012) 486–490.
[41] D.T. O'Hagan, R. van der Most, R.N. Lodaya, M. Coccia, G. Lofano, "World in motion" - emulsion adjuvants rising to meet the pandemic challenges, NPJ Vaccines 6 (1) (2021) 158.
[42] S. Akira, K. Takeda, Toll-like receptor signalling, Nat. Rev. Immunol. 4 (7) (2004) 499–511.
[43] S. Akira, S. Uematsu, O. Takeuchi, Pathogen recognition and innate immunity, Cell 124 (4) (2006) 783–801.
[44] G.M. Barton, J.C. Kagan, A cell biological view of Toll-like receptor function: regulation through compartmentalization, Nat. Rev. Immunol. 9 (8) (2009) 535–542.
[45] V. Mata-Haro, C. Cekic, M. Martin, P.M. Chilton, C.R. Casella, T.C. Mitchell, The vaccine adjuvant monophosphoryl lipid A as a TRIF-biased agonist of TLR4, Science 316 (5831) (2007) 1628–1632.
[46] Y.Q. Wang, H. Bazin-Lee, J.T. Evans, C.R. Casella, T.C. Mitchell, MPL adjuvant contains competitive antagonists of human TLR4, Front. Immunol. 11 (2020), 577823.